Temperature measurement of laser-cooled atoms using vacuum Rabi splitting

Tridib Ray,* Arijit Sharma, S. Jyothi, and S. A. Rangwala†
Raman Research Institute, Light and Matter Physics, Sadashivanagar, Bangalore 560080, India
(Received 27 February 2013; published 26 March 2013)

We laser cool rubidium atoms to form a magneto-optical trap, within a Fabry-Perot cavity, and demonstrate strong coupling of the cold atoms to the cavity. The coupling strength is measured using the vacuum Rabi frequency splitting (VRS) of transmitted, cavity-coupled light on atomic resonance. The VRS is measured for two- and three-level atomic systems and the atom-cavity-coupling strength for each system is determined. By allowing the laser-cooled atoms to expand for different times and measuring the corresponding VRS, we determine the number of atoms overlapped with the cavity mode as a function of time. This time-of-flight of atoms from the cavity permits the measurement of the temperature of the laser-cooled atoms. Finally, the need for this technique and its utility is discussed.

DOI: 10.1103/PhysRevA.87.033832 PACS number(s): 37.30.+i, 42.50.Nn

I. INTRODUCTION

The interaction of atoms with the quantized electromagnetic field is studied in atom-cavity-coupled systems. The cavity defines the boundary conditions for the electromagnetic modes that can survive within. When the cavity is loaded with near resonant atoms, the emission properties of the atoms and the cavity transmission are modified in the presence of each other [1,2]. Two regimes of interest are (a) weak coupling and (b) strong coupling between the cavity and the atoms. These regimes are categorized using three independent parameters: the free space atomic spontaneous emission decay rate γ, the photon decay rate from the empty cavity κ, and the single atom-cavity coupling g_0. In the weak-coupling regime, when $\gamma > g_0 > \kappa$, the spontaneous emission rate of the atom into the cavity mode can be enhanced or inhibited depending on the system parameters. For a single atom, the strong-coupling regime is achieved when $g_0 > (\gamma,\kappa)$ [3]. Here the atom-cavity coupling lifts the degeneracy in the atom-photon dressed state manifold. This lifting of degeneracy is detected by measuring the near atomic resonance transmission profile of the atom-cavity-coupled system. A split in the transmission profile of $2g_0$ is observed and identified as the vacuum Rabi split (VRS) [4–6]. When N_C atoms collectively couple to a single mode of the cavity, the coupling strength is enhanced by a factor of $\sqrt{N_C}$ and the new eigenstates are separated by the effective coupling strength $2g_0\sqrt{N_C}$ [7–9].

The fact that a splitting in the frequency of transmitted light through a cavity can be engineered and detected when a few thousand atoms occupy the cavity mode, opens up the possibility of using such a system as a detector for atomic processes. Since the mode volume of the cavity is generally small and very well characterized, detection of changes in atom number are enabled with pinpoint accuracy. Increasingly, experiments are being constructed which mix different species [10–14], and allow for interactions between them. Should these interactions lead to changes in atom numbers, a strongly coupled atom-cavity system could enable sensitive and accurate detection of atom loss with small atom numbers. In atomic physics, the magneto-optical trap (MOT) is the common base for physics with ultracold atoms. Therefore, constructing a strongly coupled atom-cavity system, with atoms in a MOT, is a perfect first choice for a detector using atoms. Below we explore how MOT atoms can be collectively strongly coupled to a cavity and establish the essential framework for the detection process described above.

In the present article we study the coupling of laser-cooled atoms in a MOT to a moderate finesse Fabry-Perot cavity. The finesse of the cavity is insufficient to couple individual atoms strongly to the cavity mode. However, a fraction of the atoms in the MOT can couple collectively to the cavity to achieve strong coupling [15]. Vacuum Rabi splitting is demonstrated as an experimental manifestation of atom-cavity strong coupling, and its variation with an effective number of atoms (N_C) coupled to the cavity mode is shown. The system is studied for a closed two-level case as well as with open three-level atomic systems. In both cases the results agree well with the Tavis-Cummings model [16,17]. This allows one to reliably determine N_C from experimentally measured VRS. Switching off the cooling and repumper lasers sequentially prepares the atomic population in one ground state and stops the cooling process, allowing the MOT to expand. Measuring VRS and hence the number of atoms coupled to the cavity at different delay, permits the determination of the MOT expansion rate, and hence the initial temperature of the MOT atoms. Good agreement is found between temperature measurement of the cold atoms using different polarization states of the probe laser. Statistical errors are documented and systematic errors are evaluated. We conclude with a discussion on the significance of such a measurement and its utility as a general technique of temperature measurement for multispecies experiments [10–14,18].

II. EXPERIMENTS

A. Experimental system

The experiment comprises a MOT of ^{85}Rb (rubidium) atoms at the center of a symmetric, near confocal Fabry-Perot (FP) cavity, enclosed in an ultrahigh vacuum chamber. The setup is illustrated schematically in Fig. 1. The ^{85}Rb MOT is formed using three mutually orthogonal pairs of counter-

*tray@rri.res.in
†sarangwala@rri.res.in

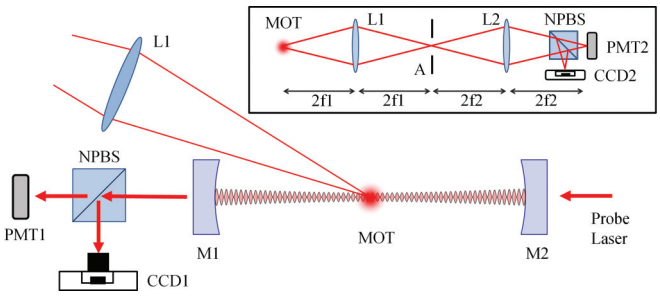

FIG. 1. (Color online) Schematic of the experimental setup. M1,M2: cavity mirrors; PMT1,PMT2: photomultiplier tubes; L1,L2: lens, NPBS: nonpolarizing beam splitter. Here the Fabry-Perot cavity is shown, with the MOT at the center, intersecting the cavity mode. The transmitted probe light from the cavity is divided and detected by PMT1 and CCD1. Fluorescence light from the MOT atoms is collected on lens L1, spatially filtered (as shown in inset), and detected by the PMT2-CCD2 setup.

propagating laser beams intersecting at the geometrical center of the vacuum chamber. Each beam is ~ 8 mm in diameter and $\sim -2\Gamma$ detuned from the $5S_{1/2}(F=3) \leftrightarrow 5P_{3/2}(F'=4)$ transition, where Γ is the natural linewidth of the transition. The repumping light is on resonance with the $5S_{1/2}(F=2) \leftrightarrow 5P_{3/2}(F'=3)$ transition and copropagating with the cooling laser beams. A total 20 mW of cooling and 2 mW of repumper power is equally distributed over the six laser beams. The gradient magnetic field at the center is ~ 22 G/cm, so as to create a small and dense MOT [19]. This magnetic field is created by passing a current of a few ampere through a pair of anti-Helmoltz coils. This increases the fraction of MOT atoms effectively coupled to the cavity mode. Rubidium atoms are derived from a getter source. The atom emission rate and hence the number of atoms loaded into the MOT from the ambient vapor can be controlled by the current through the getter source.

The MOT fluorescence is spatially filtered (as shown in the inset of Fig. 1) using a $2f-2f$ lens combination. The viewport of the chamber defines the solid angle of the light collection. The spatially filtered light is then divided by a nonpolarizing beam splitter (NPBS). One component is incident on a CCD camera (CCD2), imaging the MOT. The other component is incident onto a calibrated photomultiplier tube (PMT2) which returns a current value proportional to the incident light. The photon flux, scattered by the atoms in the MOT, is measured by the PMT signal. Given the atom-photon scattering rate [20] for the intensity and detuning of the cooling laser, the total number of atoms in the MOT is determined.

The cavity consists of two mirrors with radius of curvature $R = 50$ mm mounted at a separation of $L \approx 45$ mm. The cavity length can be modulated by application of a suitable voltage to a piezoelectric stack on which one of the mirrors is mounted. The reflectivity r of each mirror is $\geqslant 0.9997$ at $\lambda = 780$ nm. The linewidth of the cavity, without atoms, is measured by creating 20 MHz sidebands on the laser light coupled into the cavity and detected in transmission as the cavity length is scanned. A series of these measurements permits the determination of the cavity linewidth at this frequency as $1.4 \pm (0.2)$ MHz, which corresponds to the finesse of ≈ 2350. Light transmitted out of the cavity is detected once again by splitting it using a NPBS. One half of the light is detected by PMT1, while the other is imaged on CCD1, to monitor the spatial mode built up within the cavity.

In order to determine the mode volume V_{CM} and the waist w_0, one needs to accurately measure the length L of the cavity. The frequency spacing between a specific $\mathrm{TEM}_{\mathrm{mn}}$ and the next higher order transverse mode is given by [21]

$$\Delta\nu_{\mathrm{tr}} = \nu_{m,n} - \nu_{m,n+1} = \frac{c}{2\pi L}\cos^{-1}\left(1-\frac{L}{R}\right), \qquad (1)$$

where $c/2L$, the free spectral range (FSR) of the cavity, is the frequency spacing between two adjacent TEM_{00} modes. The exact length of the cavity is obtained by measuring $\Delta\nu_{\mathrm{tr}}$ using the sideband technique, giving the precise value of $L = 45.7$ mm. The waist of the TEM_{00} mode at the center is $w_0 = 78\ \mu$m.

Alignment of the MOT center with the cavity axis is very crucial for this experiment. The position of the MOT can be changed by adjusting the anti-Helmohltz coil pair. With basic alignment, a fraction of the MOT fluorescence is coupled out of the cavity. The spatial structure of the modes is monitored on CCD1. Fine alignment is achieved iteratively, by maintaining radial symmetry of the higher order modes coupled out of the cavity as well as the symmetric Gaussian spatial profile of the MOT (imaged on CCD2).

B. Experimental procedure

The MOT is first loaded to number saturation. The cavity length is tuned so that it is resonant with one of the atomic transition frequencies $\omega_{34,33,32}$ corresponding to $5S_{1/2}$-$5P_{3/2}$, $F = 3 \leftrightarrow F' = 4,3,2$ (shorthand notation: 3-4′,3′,2′) transitions shown in Fig. 2. The atoms are then optically pumped by sequentially switching off the cooling and repumping lasers to create a nonfluorescing atomic population in the $5S_{1/2}\,(F=3)$ atomic state. The experimental sequence is shown in Fig. 3. A very weak probe laser light is coupled into the TEM_{00} mode of the cavity and scanned across the atomic transition frequency. The transmitted light from the cavity is detected as illustrated in Fig. 1. The transmitted spectra shows a double peak structure around the atomic resonance (as shown in the inset of Fig. 3) when strong coupling is achieved. It is important to note that the 3-4′ is a closed cycle transition but the 3-3′ and 3-2′ are not. When these open transitions are being probed, no VRS is seen, unless the weak repumping light is also kept on to recycle back the atoms to the $5S_{1/2}, F = 3$ ground state.

C. Conditions for atom-cavity strong coupling

Condition for strong coupling for a single atom to a single mode of a cavity is $g_0 > (\gamma,\kappa)$ [6,8]. The single atom-cavity coupling g_0 is written as [1,4]

$$g_0 = \sqrt{\frac{\mu^2\omega_{\mathrm{at}}}{2\hbar\epsilon_0 V_{\mathrm{CM}}}}, \qquad (2)$$

where μ is the transition dipole matrix element between the participating states, ω_{at} is 2π times the transition frequency, ϵ_0 is the permittivity of free space, $\hbar$ is the reduced Planck's constant, and $V_{\mathrm{CM}} \sim \pi w_0^2 L/2$ is the cavity mode volume. In our experiment, given the relatively large mode volume

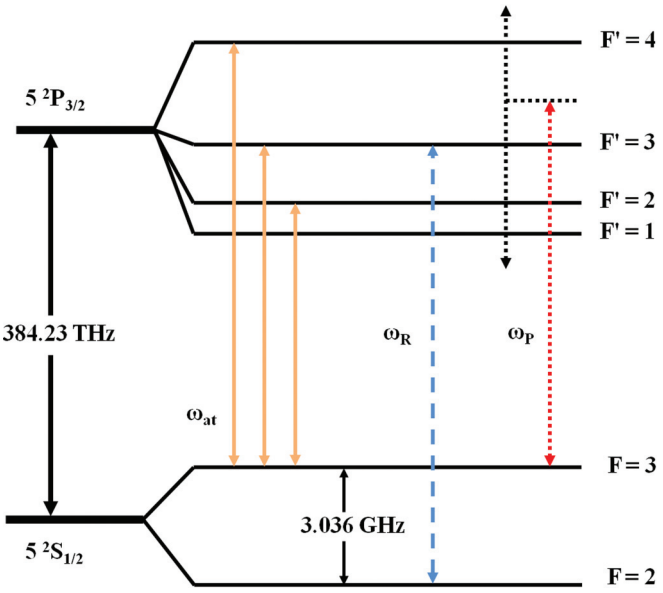

FIG. 2. (Color online) The energy-level diagram for ^{85}Rb relevant to the present experiment. The solid orange lines show the dipole allowed atomic transitions (ω_{at}) connecting the $F = 3$ ground state. VRS is observed across one of these transitions. Cooling laser is $\sim -2\Gamma$ red detuned from (ω_{34}). The dashed blue line represents the repumping laser frequency. The dotted red arrow represents the probe laser scanning across (ω_{at}).

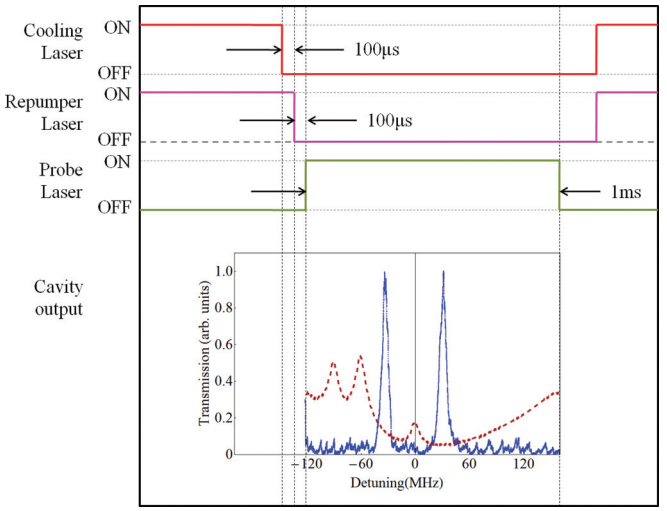

FIG. 3. (Color online) Timing sequence diagram illustrates the procedure for measurement of the VRS on the $F = 3 \leftrightarrow F' = 4$ transition. At first the cooling laser is switched off, preparing the atoms in the $F = 3$ state. The repumper laser pumps the small fraction of atoms in the $F = 2$ state back to the $F = 3$ state and then switches off after 100 μs. After another 100 μs, the probe laser is turned on and scanned across the ω_{34} within the next 1 ms. During the measurement, the cavity is tuned to ω_{34}. VRS is observed across ω_{34}. Cooling and repumper lasers are switched on immediately after the probe laser is switched off. The whole sequence is repeated at 12.5 Hz. In the bottom figure, the solid trace shows a typical VRS spectrum, while the dashed trace exhibits a part of the Rb saturation absorption spectrum, which serves as a frequency reference.

required by geometric constraints to accommodate the MOT, the single atom-cavity-coupling strength is too small to allow strong coupling. However, collective strong coupling can easily be achieved by increasing the number of MOT atoms (N_C) coupled with the cavity mode. In this scenario, the separation between the new eigenstates is given by [7–9]

$$\text{VRS} = 2g_0\sqrt{N_C}. \tag{3}$$

Depending on the strength of the dipole transition of the two participating states, the minimum number of atoms required to achieve strong coupling changes. In the present experiment, the MOT gradient magnetic field is on throughout the experiment. In this case the atomic dipoles of the cavity mode atoms will have projections along all three directions depending on their positions. As a result, over the entire atomic ensemble in the cavity mode, the probe light of any given input polarization can be considered to have a nearly isotropic polarization, seen by the atomic dipoles. So we utilize the transition dipole matrix for isotropically polarized light [22], in estimating the theoretical value of g_0, using Eq. (2). The calculated values for g_0 are 142, 93, and 50 kHz corresponding to ω_{34}, ω_{33}, and ω_{32}, respectively. The typical $N_C(\sim 10^4)$ in the present setup is therefore sufficient to achieve a detectable strong-coupling VRS for these transitions.

D. Experiments and results

The number of atoms in the MOT is determined by measuring the fluorescence collected on PMT2. The density profile of the MOT is determined by fitting a symmetric Gaussian to the image of the MOT captured by CCD2. The fitted normalized Gaussian distribution with the measured full width at half maximum (FWHM), multiplied by the total number of atoms captured in the MOT gives the number density distribution $\rho(x,y,z)$ of the MOT. The field distribution of the TEM_{00} mode of the cavity is given by [21]

$$\psi(x,y,z) = \frac{w_0}{w(z)}\exp\left[-\frac{x^2+y^2}{w^2(z)}\right]\sin(kz), \tag{4}$$

where $\hat{z}$ is the cavity axis and $w(z)$ is the width of the cavity mode at a distance z from the cavity center. So the effective number of atoms coupled to the cavity mode is given by

$$N_C = \int_{\tilde{V}} \rho(x,y,z)\psi^2(x,y,z)dx\,dy\,dz, \tag{5}$$

where the integration volume $\tilde{V} \gg V_{\text{MOT}}$ (the MOT volume).

The variation of VRS as a function of N_C, when the cavity length is tuned to the atomic resonance (ω_{at}), is measured. In such a measurement only the 3-4′ transition is closed and therefore is a two-level system, whereas the 3-3′,3-2′ transitions are open, allowing the atom from the excited 3′,2′ state to decay to the $5S_{1/2}(F = 2)$ state, making these effectively three-level systems. This then constitutes a loss channel from the excited state, and no VRS is detected in this case, unless this loss channel is plugged by keeping the weak repumping light on. When this is done, VRS can be observed around the 3-3′,2′ transitions also. VRS measurements were made across the 3-4′ transition with the repumper on and off to compare the difference. These measurements are illustrated in Fig. 4.

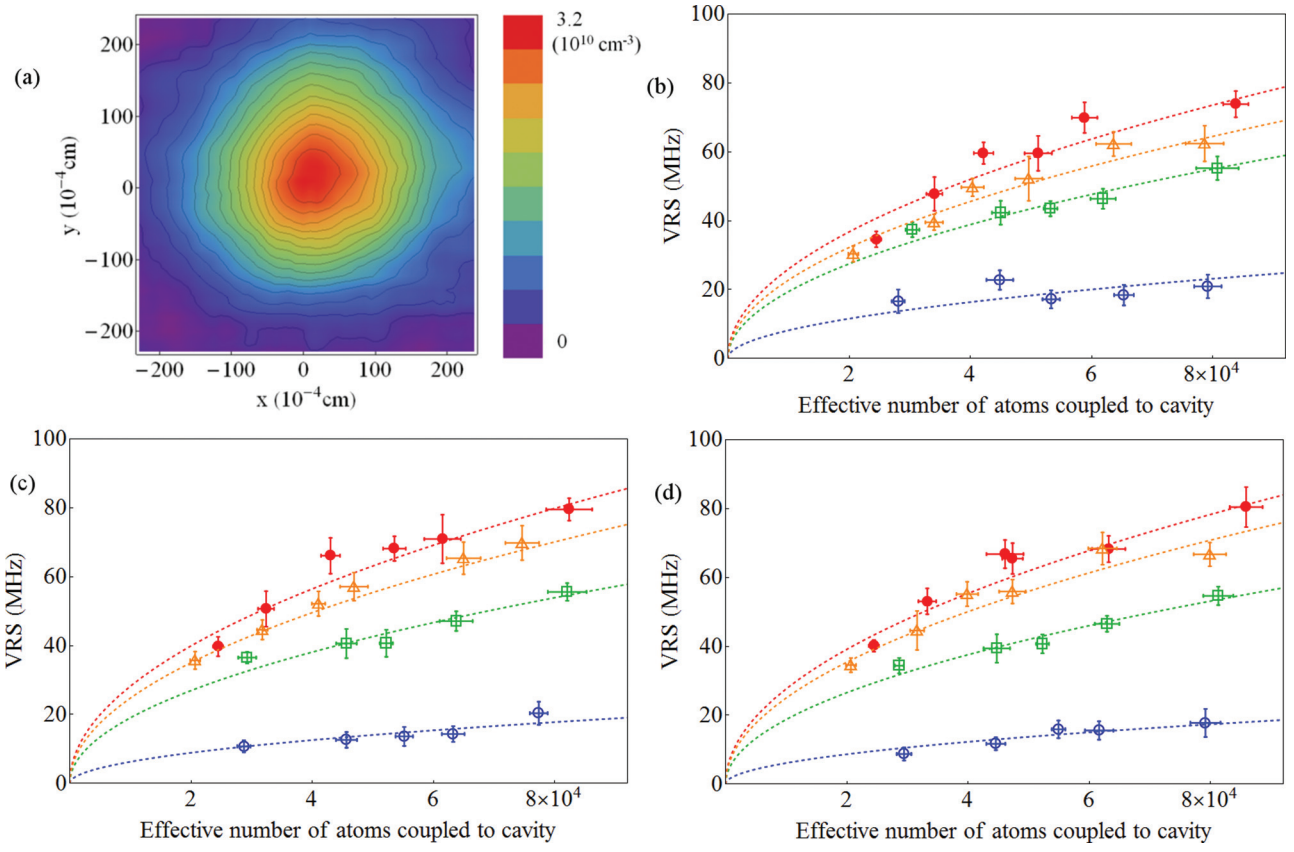

FIG. 4. (Color online) (a) The MOT density profile. The FWHM is 235 μm and peak number density is $3.2 \times 10^{10}/\text{cm}^3$. Panels (b), (c), and (d) illustrate VRS as a function of atom number (N_C) in the cavity mode. Red disks, orange triangles, green squares, and blue circles represent VRS across ω_{34} with repumper on, ω_{34} with repumper off, ω_{33}, and ω_{32} transitions, respectively. The error bars are the statistical errors representing one standard deviation. The dashed lines are the fits to each set of data by $2g_0\sqrt{N_C}$, from which the value of g_0 can be determined for each transition. Data for the linear polarization (LinP) (b), left circular polarization (LCP) (c), and right circular polarization (RCP) (d) of the probe laser has been shown. Fit value and errors to the fits have been summarized in Table I.

To measure the atom-cavity coupling, the number of atoms in the cavity mode volume is varied by changing the getter current in a systematic way. The variation in the atom number is measured from the MOT fluorescence. The corresponding change in VRS is shown in Fig. 4. Fit of the data by Eq. (3) measures the g_0 for each transition. The results are given in Table. I.

Clearly, when repumping is off, the measured value of $g_{0:34}$ is lower than when the repumping laser is on. This is attributed to a loss of atoms during the experiment, into the $F = 2$ dark state. When the repumping laser is on, the atoms are pumped back into the $F = 3$ ground state, and participate in atom-cavity coupling. For the $g_{0:33}$ and $g_{0:32}$ measurements, the presence of the repumping light is a must. We also note that the measured values of g_0 are mostly insensitive to the polarization state of the probe light, as seen in Table I, and discussed earlier. For further measurements using VRS, we use the experimental values of g_0, as these will incorporate any birefringence due to the cold-trapped atoms and the cavity mirrors.

TABLE I. Experimentally measured values of g_0, the atom-cavity coupling constant, for the various cases of probe polarization and transitions considered. R and NR in parentheses represents a measurement with repumping or no repumping, respectively. The standard deviation errors to the fits in Fig. 4 are shown for each measurement.

Atom-cavity coupling	LinP (kHz)	LCP (kHz)	RCP (kHz)
$g_{0;34}$(NR)	$114 \pm (2.6)$	$124 \pm (2.9)$	$125 \pm (3.3)$
$g_{0;34}$(R)	$130 \pm (3.9)$	$141 \pm (3.2)$	$138 \pm (3.7)$
$g_{0;33}$(R)	$97 \pm (2.1)$	$95 \pm (2.4)$	$94 \pm (1.8)$
$g_{0;32}$(R)	$41 \pm (3.5)$	$31 \pm (1.7)$	$31 \pm (1.3)$

Having determined the experimental atom-cavity-coupling constants, we now use them to measure the MOT temperature. Since the duration of the measurement is long, the getter source is kept at a low current value, so that there is no buildup of ambient vapor pressure during the experiment. This means working with a small MOT and therefore smaller VRS. It also implies that the measurements need to be made across ω_{34}. The experimental sequence remains similar to the one described above, with one exception. The time interval between the switching off of the cooling laser and the probing of the cavity mode atoms τ is now varied. Once the cooling laser is turned off, the cooling stops and the MOT undergoes ballistic expansion. The repumper laser remains on throughout the experiment. As τ increases, number density of the MOT

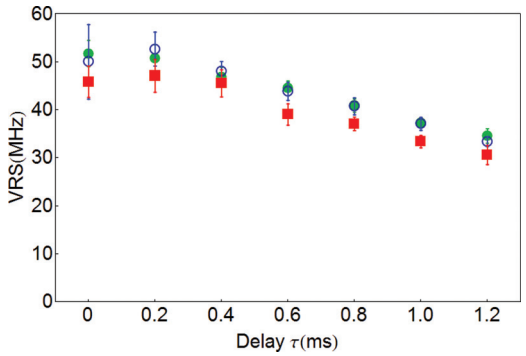

FIG. 5. (Color online) The fall in the VRS as a function of time interval τ. Due to the systematic decrease in the N_C after the cooling laser is cut, the VRS falls with increasing τ. The measurement is done across ω_{34} transition, with repumper on, for a MOT with low atom number. Red squares, green disks, and blue circles represent data for the LinP, LCP, and RCP of the probe laser, respectively. The error bars represent the statistical errors in measurement.

decreases and hence the number of atoms coupled to the cavity mode falls. The fall of N_C with τ can be probed from the measured VRS at different time intervals using Eq. (3). This behavior is illustrated in Fig. 5. Under the reasonable assumption that the expanding atom density distribution is Gaussian and symmetric, the σ for the Gaussian density distribution can be found as a function of τ. For the ballistically expanding cold cloud with initial temperature T the rate of expansion is given [23] as

$$\sigma^2(\tau) = \sigma^2(0) + \frac{k_B T}{m}\tau^2, \tag{6}$$

where k_B is the Boltzmann constant and m the mass of the ^{85}Rb atom. Figure 6 shows experimentally measured $\sigma^2(\tau)$ as a function of τ^2. The linear slope on this plot is proportional to the temperature of the MOT (T_{MOT}). We note that the intercept $\sigma^2(0)$ very accurately measures the initial spatial size of the MOT, emphasizing the robustness of the time- of-flight measurement technique demonstrated here. The experiment was performed across ω_{34} with a linearly polarized (LinP), left (LCP) and right (RCP) circularly polarized probe laser,

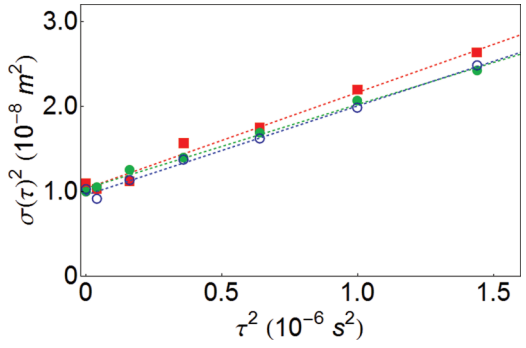

FIG. 6. (Color online) The plot of the square of the width of the released distribution of atoms as a function of the square of the time interval between the release and the measurement. The slope of the linear fit gives the MOT temperature and the y intercept the initial size of the MOT. Red squares, green disks, and blue circles represent the data for the LinP, LCP, and RCP of the probe laser, respectively.

TABLE II. Measured temperature of the cold atomic cloud for the linear (LinP), left and right circularly polarized (LCP and RCP) probe light and the corresponding measured g_0 value. One standard deviation errors are shown for each temperature value.

Probe polarization	g_0 (kHz)	T_{MOT} (μK)
LinP	130	115 ± 9.4
LCP	141	101 ± 5.7
RCP	138	107 ± 7.3

with the repumping light on. The MOT temperatures obtained are given in Table II, along with the one-sigma errors to the respective fits. The combined temperature of the MOT obtained from all three polarization states of the probe laser is $T_{\mathrm{MOT}} = 107.7 \pm 7.5$ μK, which is reasonable for the small MOT in the experiment.

Two sources of systematic errors in this method for temperature determination are the gradient magnetic field and gravity. It must be noted that the gradient magnetic field has not been turned off during MOT expansion. The field causes acceleration or deceleration of the atoms, depending on their m_F state and direction of velocity. The effect of the magnetic field on $\sigma^2(\tau)$ is $\sim\pm(v_{\mathrm{at}} a\tau^3)$, where a is the magnitude of acceleration or deceleration of the atom in the magnetic field and v_{at} is the initial atomic velocity. Maximum a in this case is ~ 15 m/s^2 leading to a worst case error $\sim 9\%$, in the measurement of $\sigma^2(\tau)$. In the current experiment, where the potential energy of the atoms in the magnetic field is much smaller than their kinetic energy, the contribution can be neglected. The effect of gravity is to shift the center of the atomic cloud with time, causing the overlap of the MOT and the cavity mode to reduce faster. The present experiment was performed for a very small time of expansion so that the effect of gravity can be safely be neglected [24] for the measured temperature limit. It is estimated that the error in the measurement due to gravity would cause a maximum error of ~ 20 kHz in VRS for the maximum τ, which is well within the statistical error bars of the measured VRS, and is therefore not corrected for.

III. DISCUSSION

MOT densities are low enough for the atoms to be noninteracting and there is little contribution from any potential energy or interaction terms in the present single MOT experiment. Therefore the method does measure the temperature of the MOT. When one considers loading cavities with mixtures of interacting cold species in their respective traps, the technique can be adapted to measure the interspecies interaction [18], with minimal perturbation of the overall system. As an example one could use this method for the determination of ion-atom interactions and atom temperature in mixed ion-atom systems [10–14]. The fact that the measurement takes place within a millisecond, allows for repeated and frequent measurement. Since a cavity supports only a narrow band of frequency, it can be used to selectively interrogate the properties of a specific species in atom mixture experiments, to be performed in the near future. The demonstration that

the atom-cavity system can be pushed into strong coupling and this can be detected whether we probe on a open or a closed transition allows for flexibility in detection. This is significant because in the presence of other fluorescing atoms or ions, the frequency of the probe light for one set of atoms might coincide with resonant buildup from fluorescing atoms or ions of the other species, in one of the many transverse cavity modes, and saturate the detector. If several options are available for interrogation, as demonstrated here, this problem can be avoided to a very good extent. For atom-cavity systems, this technique therefore represents a versatile method for measurement of temperature and other properties of cold atomic ensembles. A related demonstration of collective strong coupling of an ion crystal to a FP cavity of similar finesse has been recently demonstrated [25,26].

IV. CONCLUSIONS

In this article we have demonstrated the formation of a MOT of Rb atoms within a Fabry-Perot cavity. The cold atoms within the cavity are shown to strongly couple to the TEM_{00} mode of the cavity. The atom-cavity-coupling factor is measured for several atomic transitions by a measurement of the VRS. It is seen that for the closed two-level system, a nonzero VRS is measured, whether the atoms are being repumped or not. However, for the open three-level systems, it is imperative to have the repumping on throughout the measurement, in order to see a nonzero VRS. It is determined that the VRS measurements with the repumping on are quite consistent, and these are used to measure the temperature of the MOT, by switching off the MOT cooling, measuring the VRS and therefore the atom number in the cavity, as a function of time. It is shown that the polarization state of the probe laser does not alter the measured value of the MOT temperature. The method developed here therefore is an interesting approach, which can be used for a variety of measurements on cold gas mixtures.

ACKNOWLEDGMENTS

The authors gratefully acknowledge the RRI workshop for the manufacturing of the experimental apparatus and RAL for electronics support.

[1] *Cavity Quantum Electrodynamics*, edited by P. R. Berman (Academic Press, New York, 1994).
[2] S. Haroche and J. M. Raimond, *Exploring the Quantum: Atoms, Cavities, and Photons* (Oxford University Press, Oxford, 2006).
[3] E. Jaynes and F. Cummings, Proc. IEEE **51**, 89 (1963).
[4] J. J. Sanchez-Mondragon, N. B. Narozhny, and J. H. Eberly, Phys. Rev. Lett. **51**, 550 (1983).
[5] R. J. Thompson, G. Rempe, and H. J. Kimble, Phys. Rev. Lett. **68**, 1132 (1992).
[6] J. J. Childs, K. An, M. S. Otteson, R. R. Dasari, and M. S. Feld, Phys. Rev. Lett. **77**, 2901 (1996).
[7] G. S. Agarwal, Phys. Rev. Lett. **53**, 1732 (1984).
[8] M. G. Raizen, R. J. Thompson, R. J. Brecha, H. J. Kimble, and H. J. Carmichael, Phys. Rev. Lett. **63**, 240 (1989).
[9] Y. Zhu, D. J. Gauthier, S. E. Morin, Q. Wu, H. J. Carmichael, and T. W. Mossberg, Phys. Rev. Lett. **64**, 2499 (1990).
[10] A. T. Grier, M. Cetina, F. Oručević, and V. Vuletić, Phys. Rev. Lett. **102**, 223201 (2009).
[11] W. G. Rellergert, S. T. Sullivan, S. Kotochigova, A. Petrov, K. Chen, S. J. Schowalter, and E. R. Hudson, Phys. Rev. Lett. **107**, 243201 (2011).
[12] F. H. J. Hall and S. Willitsch, Phys. Rev. Lett. **109**, 233202 (2012).
[13] K. Ravi, S. Lee, A. Sharma, G. Werth, and S. A. Rangwala, Nat. Commun. **3**, 1126 (2012).
[14] I. Sivarajah, D. S. Goodman, J. E. Wells, F. A. Narducci, and W. W. Smith, Phys. Rev. A **86**, 063419 (2012).
[15] G. Hernandez, J. Zhang, and Y. Zhu, Phys. Rev. A **76**, 053814 (2007).
[16] M. Tavis and F. W. Cummings, Phys. Rev. **170**, 379 (1968).
[17] M. Tavis and F. W. Cummings, Phys. Rev. **188**, 692 (1969).
[18] M. S. Santos, P. Nussenzveig, L. G. Marcassa, K. Helmerson, J. Flemming, S. C. Zilio, and V. S. Bagnato, Phys. Rev. A **52**, R4340 (1995).
[19] C. G. Townsend, N. H. Edwards, C. J. Cooper, K. P. Zetie, C. J. Foot, A. M. Steane, P. Szriftgiser, H. Perrin, and J. Dalibard, Phys. Rev. A **52**, 1423 (1995).
[20] H. Metcalf and P. Van Der Straten, *Laser Cooling and Trapping*, Graduate Texts in Contemporary Physics Series (Springer-Verlag, Berlin, 1999).
[21] A. E. Siegman, *Lasers* (University Science Books, Mill Valley, CA, 2003).
[22] D. A. Steck, *Rubidium 85 D Line Data, Revision (2.1.5)* (2012), http://steck.us/alkalidata.
[23] D. S. Weiss, E. Riis, Y. Shevy, P. J. Ungar, and S. Chu, J. Opt. Soc. Am. B **6**, 2072 (1989).
[24] P. D. Lett, R. N. Watts, C. I. Westbrook, W. D. Phillips, P. L. Gould, and H. J. Metcalf, Phys. Rev. Lett. **61**, 169 (1988).
[25] P. F. Herskind, A. Dantan, J. P. Marler, M. Albert, and M. Drewsen, Nat. Phys. **5**, 494 (2009).
[26] M. Albert, J. P. Marler, P. F. Herskind, A. Dantan, and M. Drewsen, Phys. Rev. A **85**, 023818 (2012).